LAWRENCE
LIVERMORE
NATIONAL
LABORATORY

LLNL-TR-649441

Experimental Report: ORNL Proposal ID IPTS 8937

A. Mirmelstein

February 6, 2014

Disclaimer

This work performed under the auspices of the U.S. Department of Energy by Lawrence Livermore National Laboratory under Contract DE-AC52-07NA27344.

Experimental report
ORNL proposal ID IPTS 8937, December 11-15, SNS, ORNL, TN

A. Mirmelstein, RFNC-VNIITF, Snezhinsk, Russia

I. Variation of the CeNi structure under pressure

Neutron scattering experiment was performed using fine-resolution Fermi chopper spectrometer "SEQUOIA" installed at the Spallation Neutron Source, ORNL. Although this spectrometer is designed to measure inelastic neutron scattering spectra, during experiments a signal of elastic scattering is also recorded. The coherent nuclear component of this elastic scattering provides Bragg diffraction pattern of a sample, i.e., CeNi single crystal in our case. Therefore, it is possible to follow the CeNi structural variations as a function of pressure and to register structural phase transition. Measurements were performed at the temperature of 15 K under pressure of zero (ambient pressure at 15 K), 400, 800, and 2200 bars.

It is necessary to note a circumstance strongly complicating our experiment. On the one hand, the magnetic signal, the main goal of the experiment, is very weak. Nuclear signal which forms the diffraction pattern is also suppressed due to the Ni-60 isotope used to prepare CeNi single crystal. On the other hand, the signal coming to the detector is contaminated by both elastic and inelastic components resulting from the neutron scattering from pressure cell and cryostat materials (mainly Al) surrounding the sample. Therefore, background is very high in our experiment. To subtract this background, measurements of the empty pressure cell were performed using the same experimental conditions as in the case of the cell with the sample.

Energy of incident neutrons has been chosen to be 81.8 meV (neutron wavelength λ=1 Å). *b* axis of the CeNi crystal lattice was aligned vertically, while the *a*-*c* plane of the crystal was fixed horizontally to be parallel to the horizontal scattering plane.

CeNi diffraction pattern at ambient pressure after the empty cell background subtraction is shown in Fig. 1. One can see clearly symmetrical Bragg reflections (-2 0 -2), (-2 0 2), (-2 0 0), and (0 0 2). Besides, there are intensive elastic reflections located in the "incommensurate" positions near the reciprocal lattice points (-1 0 -1), (-1 0 1), (1 0 -1), (1 0 1) and (-3 0 -1), (-3 0 1), (-1 0 -3). Most probably, these reflections originate from the residual amount of Ce_2O_3 contamination.

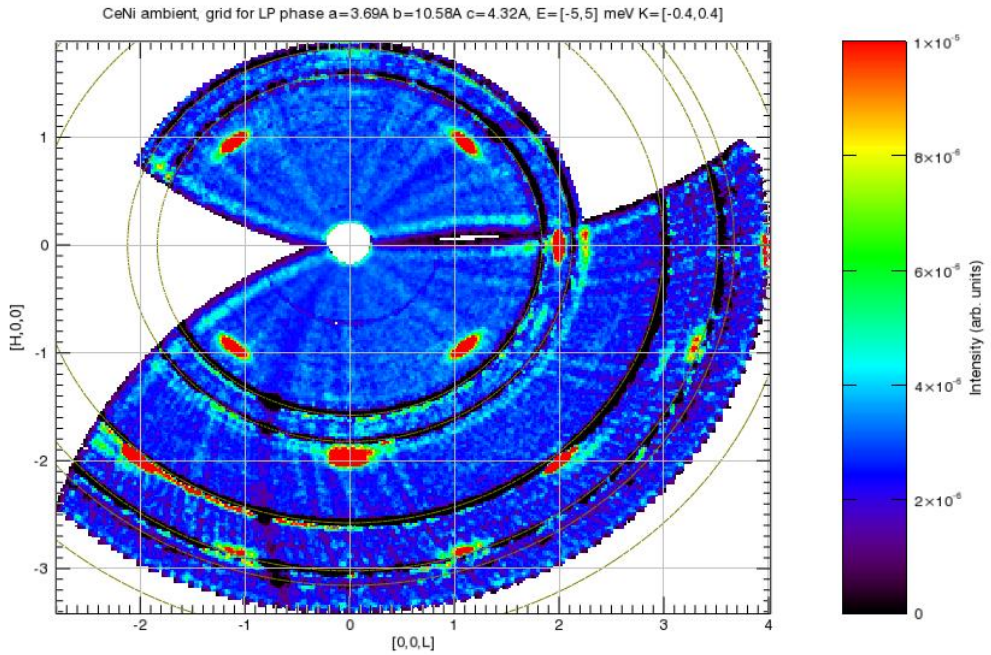

Figure 1. CeNi diffraction pattern in the reciprocal lattice plane (H 0 L) at ambient pressure. Dark circuses indicate the result of the Al elastic background subtraction. The coordination grid corresponds to the orthorhombic structure (space group Cmcm) of CeNi with the crystal lattice parameters a = 3.69 Å, b = 10.58 Å, c = 4.32 Å.

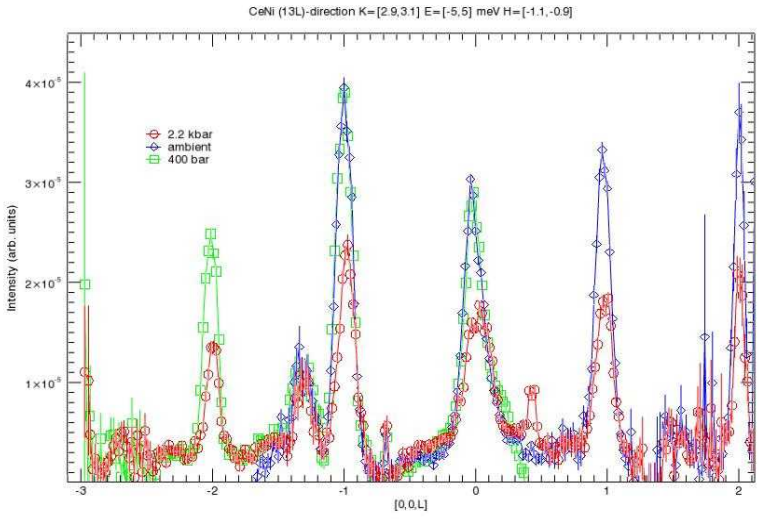

Figure 2. CeNi diffraction patter along the [-1 3 L] direction at ambient pressure and at pressures 400 and 2200 bars. (-1 3 -2), (-1 3 -1), (-1 3 0), (-1 3 1) reflection intensities of the ambient pressure phase decrease at 2200 bars. The reflection intensity in the incommensurate (-1 3 ~ 1.3) position coming, most probably, from an impurity phase, does not depend on pressure.

There are no visible structural variations at the pressure value of 400 bars, however at 2200 bars the reflection intensities of the CeNi low pressure phase decrease significantly (Fig. 2). This effect of pressure is well seen in Fig. 3 which represents the full scattering pattern in the (H 0 L) plane at 2200 bars. The coordination grid in Fig. 3 corresponds to the orthorhombic low pressure phase of CeNi, i.e. the grid is the same as in Fig. 1. Besides the low pressure phase reflections located in the regular grid positions and the reflections in the incommensurate positions, one can see weak intensities near the (-2 0 -2), (-2 0 0) и (-2 0 2) reciprocal space points. Thus, we can identify strong regular reflections as the Bragg peaks of ambient pressure phase, while more weak intensities located out of the coordination grid can be ascribed to the high pressure phase. By the other words, at 2200 bars CeNi is found to be in the region of structural phase transformation.

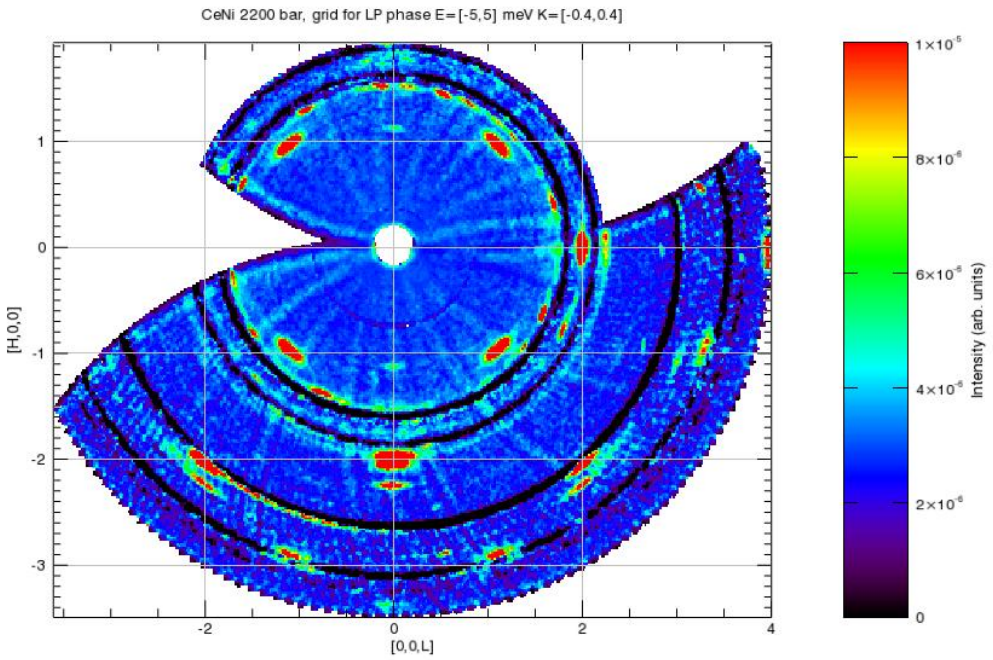

Figure 3. CeNi diffraction pattern in the reciprocal lattice plane (H 0 L) at pressure 2200 bars. The coordination grid corresponds to the ambient pressure orthorhombic structure (space group Cmcm) of CeNi with the crystal lattice parameters a = 3.69 Å, b = 10.58 Å, c = 4.32 Å (the same as in Fig. 1). Reflections in the incommensurate positions remain the same as at ambient pressure.

One can attempt to determine the symmetry of high pressure phase. For this it is necessary to find a coordination grid, or a new reciprocal lattice, which would accommodate the reflections of new phase. Figure 4 demonstrates that this is possible assuming also orthorhombic symmetry of the new phase but with different crystal lattice parameters and other directions of b and c axes, namely, the c axis of the old phase should be substituted by the b axis of the new phase and, vise verse, the b axis of the old phase should be substituted by the c axis of the new

phase. Figures 5-7 show diffraction patterns along different directions of the new reciprocal lattice. These figures confirm a possibility to describe Bragg peaks of high pressure phase in terms of the orthorhombic symmetry.

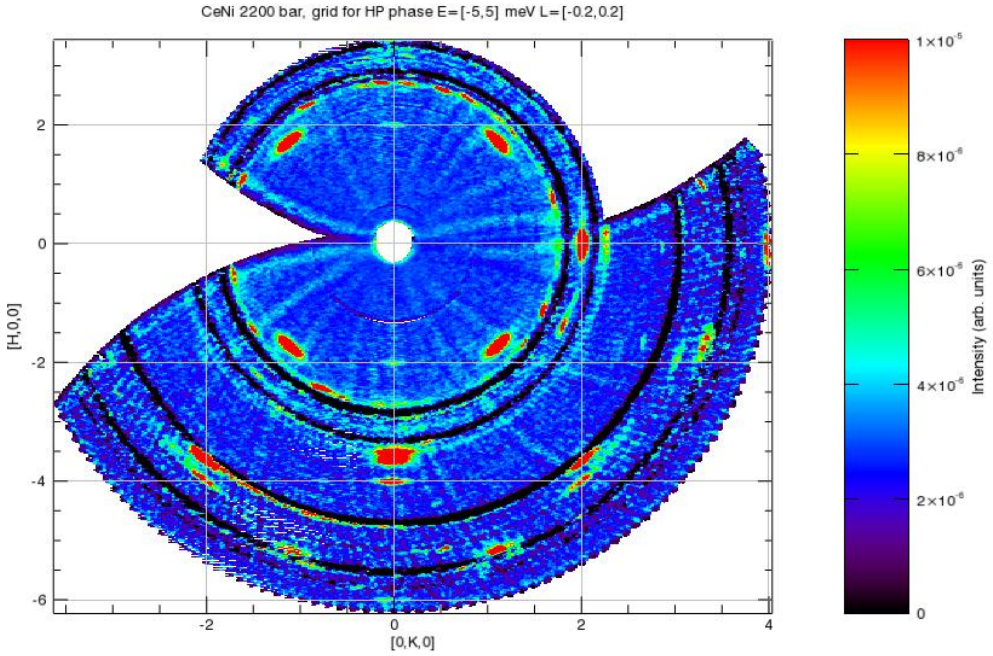

Figure 4. The same diffraction pattern of CeNi at 2200 bars as in Fig. 3 but with the new coordination grid corresponding to the new orthorhombic structure with the crystal lattice parameters a = 6.72 Å, b = 4.34 Å, c = 5.159 Å. Note that now the scattering plane is the a-b-reciprocal lattice plane (H K 0) of the high pressure phase.

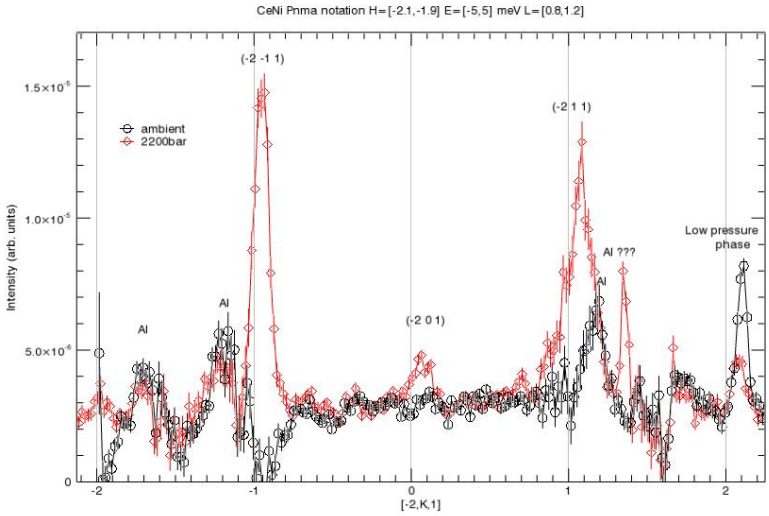

Figure 5. CeNi diffraction patterns at ambient pressure and at 2200 bars along the [-2 K 1] direction of the high pressure phase reciprocal lattice.

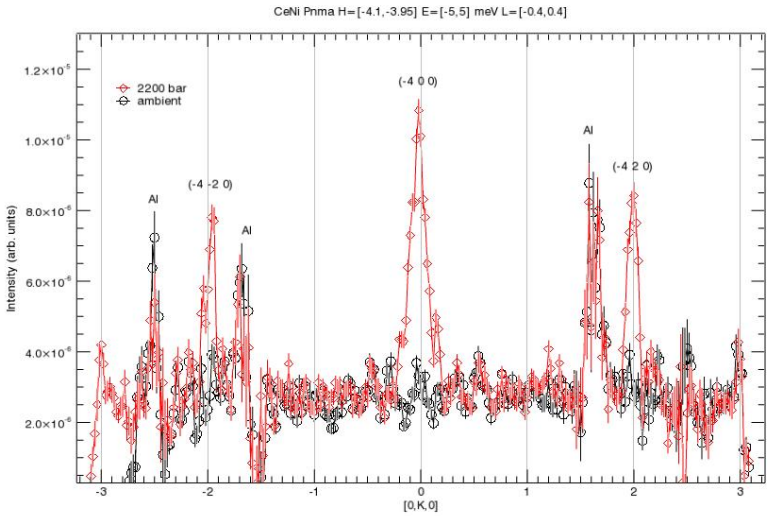

Figure 6. CeNi diffraction patterns at ambient pressure and at 2200 bars along the [-4 K 0] direction of the high pressure phase reciprocal lattice.

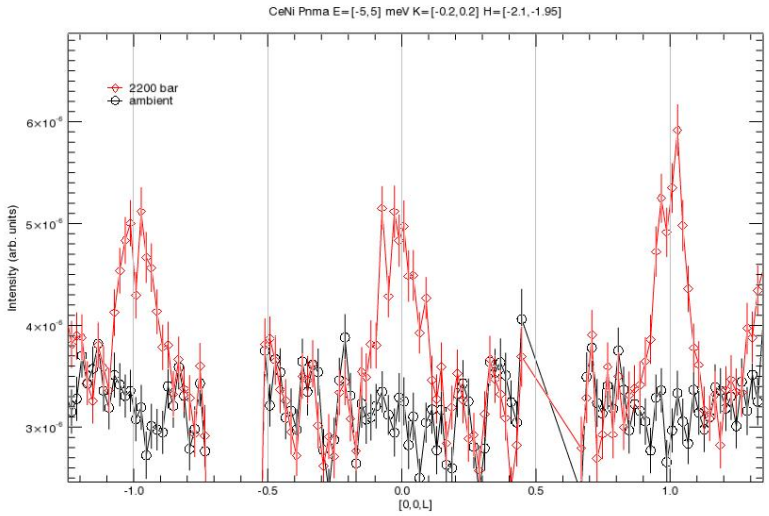

Figure 7. CeNi diffraction patterns at ambient pressure and at 2200 bars along the [-2 0 L] direction of the high pressure phase reciprocal lattice.

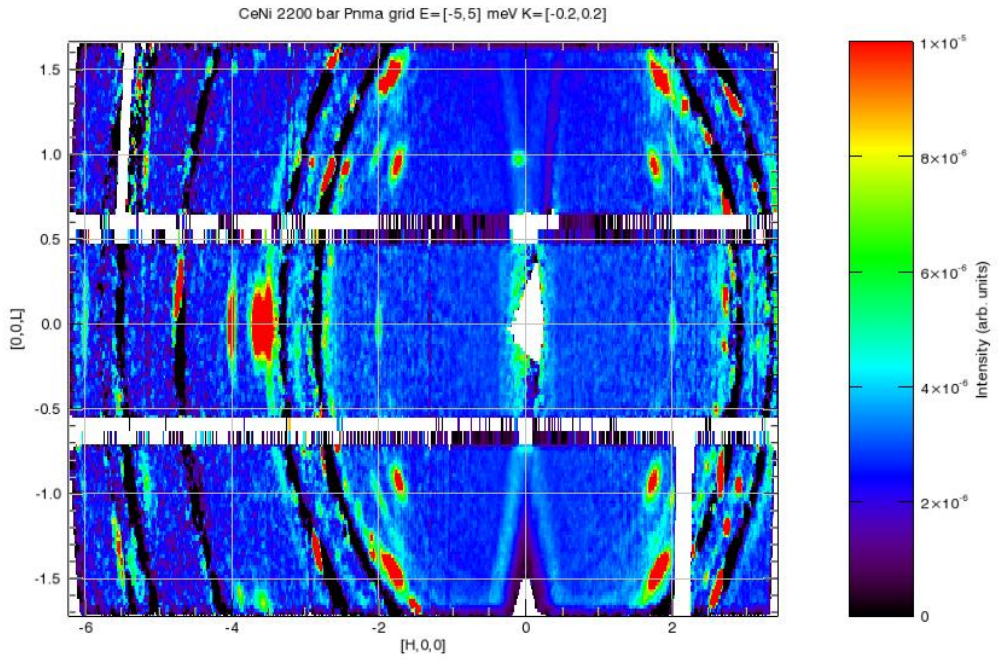

Figure 8. CeNi diffraction pattern at 2200 bars in the reciprocal lattice plane (H 0 L) of the high pressure phase. Absence of the (101) reflections is evident. Elliptical distortions of the map are produced by the data visualization program.

If in Fig. 8 there were Bragg reflections of the (1 0 1) type, it would be possible to assume the high pressure phase to have orthorhombic structure of the FeB type (space group Pnma). This structure is typical for the RNi compounds where R is the rare-earth metal from the second half of the lanthanide series, while light lanthanides, including cerium, form the crystal lattice of the CrB type (space group Cmcm) [1,2]. Both the FeB and CrB type structures contain a common structural unit, the trigonal prism, which is stacked differently to form either structure (Fig. 9). One of these structures can transform to the other directly or via a sequence of polymorphous transformations [2]. Structural definition of intermediate phases can appear extremely difficult, if a tractable problem due to numerous versions of trigonal prisms stacking. This circumstance may probably explain why for many years nobody could define the structure of CeNi high pressure phase. Some time ago we made an attempt to solve this task using neutron powder diffraction technique [3]. According to [3], the high pressure phase can be described in terms of the tetragonal symmetry, however we were not able to define the space group of high pressure phase. The results of the present study seem to disagree with our previous results. Quite possible that we simply did not have enough accuracy for the correct analysis of the diffraction experimental data in [3], but we also cannot exclude more fundamental reasons of such a discrepancy. First, a cast powder sample was studied in ref [3]. Although this sample was highly

textured it was not a single crystal. Second, the pressure was generated by sapphire anvils while in the present study helium gas was used as a pressure transmitting medium. The latter technique provides more hydrostatic compression conditions than anvils. Thus, different results of our

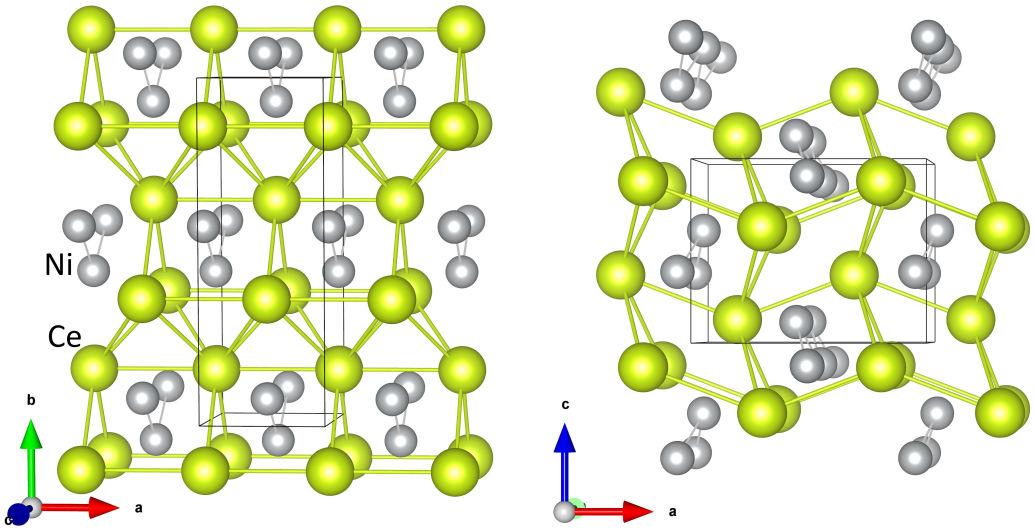

Figure 9. Left: the CrB type of structure (space group Cmcm), right: the FeB structural type (space group Pnma). Both structures contain a common structural unit, trigonal prism, which is stacked differently to form either structure.

previous and present investigations can be connected with macro-structural features of the sample under study (powder ingot vs. single crystal) as well as with the compression conditions. Obviously, we deal with interesting physics, but more experimental work is required to resolve the problem of CeNi high pressure phase structure. Andrey Podlesnyak and his colleagues plan to perform additional neutron diffraction experiment to study the pressure-induced structural phase transformation in CeNi. We will inform you about these results additionally.

II. Measurements of magnetic inelastic scattering from CeNi as a function of pressure

Due to very high background measurements of magnetic inelastic scattering from CeNi turns out to be even much more difficult task than structural investigation of this system under high pressure. Besides the inelastic background coming from Al (the main pressure cell and cryostat material) CeNi inelastic component of the measured spectrum is contaminated by the recoil scattering from He gas which fills the pressure cell and services as a pressure transmitting medium. He recoil scattering gives a rather strong inelastic signal within the energy transfer

range up to 15 meV. The intensity of recoil scattering depends on the pressure and temperature and increases with the increase in the momentum transfer Q (Fig. 0).

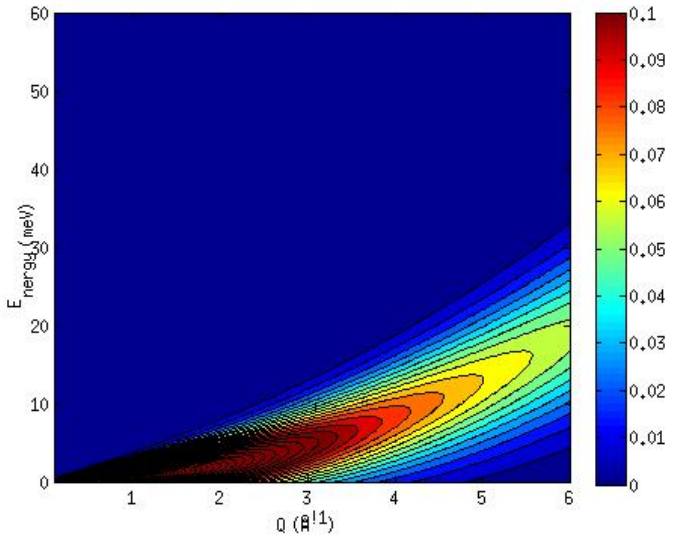

Figure 10. The map of recoil scattering form He gas at temperature 15 K.

Inelastic neutron scattering intensity is given by the double differential cross section

$$\frac{d^2\sigma}{dEd\Omega} = \frac{k_f}{k_i} S(\mathbf{Q}, E, T), \qquad (1)$$

where k_i and k_f are the magnitude of the incident and scattered wave vectors, respectively, $\mathbf{Q} = \mathbf{k_i} - \mathbf{k_f}$ is the momentum transfer, and S(**Q**,E,T) is the scattering function. In the case of magnetic scattering the scattering function is

$$S(\mathbf{Q}, E, T) = \frac{1}{2}\left(\frac{g_N r_e}{\mu_B}\right)\frac{1}{\pi}\frac{E}{1-\exp(-E/k_B T)}\chi_0(\mathbf{Q}, T)P(\mathbf{Q}, E, T), \qquad (2)$$

Since an analytical form of the spectral function P(**Q**,E,T) is unknown, Lorentzian is commonly used:

$$P(\mathbf{Q}, E, T) = \frac{1}{\pi}\frac{\Gamma/2}{(\Gamma/2)^2 + E^2}, \qquad (3)$$

where Γ is the full width at half maximum (FWHM) of this function. Note that in the case of a powder sample magnetic scattering function turns out to be averaged over the directions of wave vectors, and the dependence of Eq. (2) on the momentum transfer can be written as

$$S(Q, E, T) \sim \frac{E}{1-\exp(-E/k_B T)}\chi(T)\,|f(Q)|^2\,\frac{\Gamma/2}{(\Gamma/2)^2 + E^2},$$

where $\chi(T)$ is the bulk magnetic susceptibility, and f(Q) is the magnetic form factor. For nuclear scattering the cross section is generally proportional to the momentum transfer squared Q^2. Different momentum transfer dependences allow to separate nuclear and magnetic scattering. Nuclear scattering dominates at high momentum transfer while magnetic scattering is best observable at low Q.

Because of extremely weak inelastic intensity obtained for CeNi in our experiment after background (pressure cell without CeNi sample) subtraction, below we consider "powder averaged" scattering functions for the low (0 to 2 $Å^{-1}$), intermediate (2 to 4 $Å^{-1}$), and high (4 to 6 $Å^{-1}$) momentum transfer (Fig. 11-13). These spectra can hardly be interpreted. For example, the low-Q spectra show some features at energy transfer between 15 and 30 meV (Fig. 11) which can be preliminary associated with the CeNi phonon contribution. If so, similar featureы are expected to be enhanced at high momentum transfer. Instead, we see almost flat and very weak intensity within this energy range at high momentum transfer (Fig. 13). Strong scattering below 10 meV in Fig. 11, which grows with increase in pressure, most probably, is due to helium. However at the higher momentum transfers r (Fig. 12 and 13) this scattering seems to be much broader in energy than expected for the helium excitations. The CeNi and Al phonon densities of states have an energy cutoff at about 24 meV [4] and about 40 meV [5], respectively. Therefore, above 40 meV the inelastic scattering should be mainly of magnetic origin. However, the origin of a rather sharp and pressure-independent maximum slightly above 70 meV is questionable. It may result from the multiphonon scattering, but this is not evident and should be verified

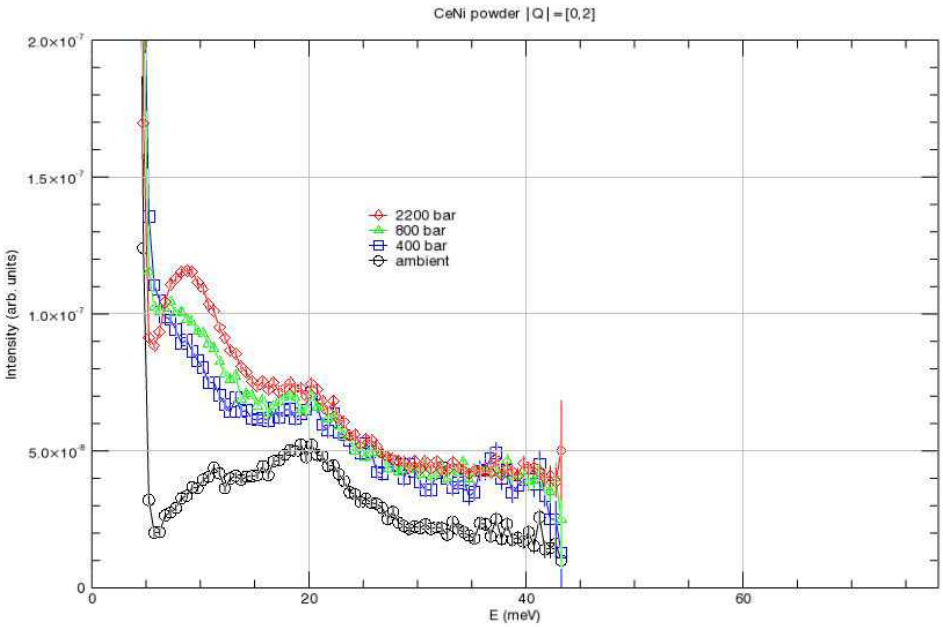

Figure 11. Scattering function S(E) for CeNi averaged over the momentum transfer values 0 < |Q| 2 $Å^{-1}$ at T = 15 K and different pressure values.

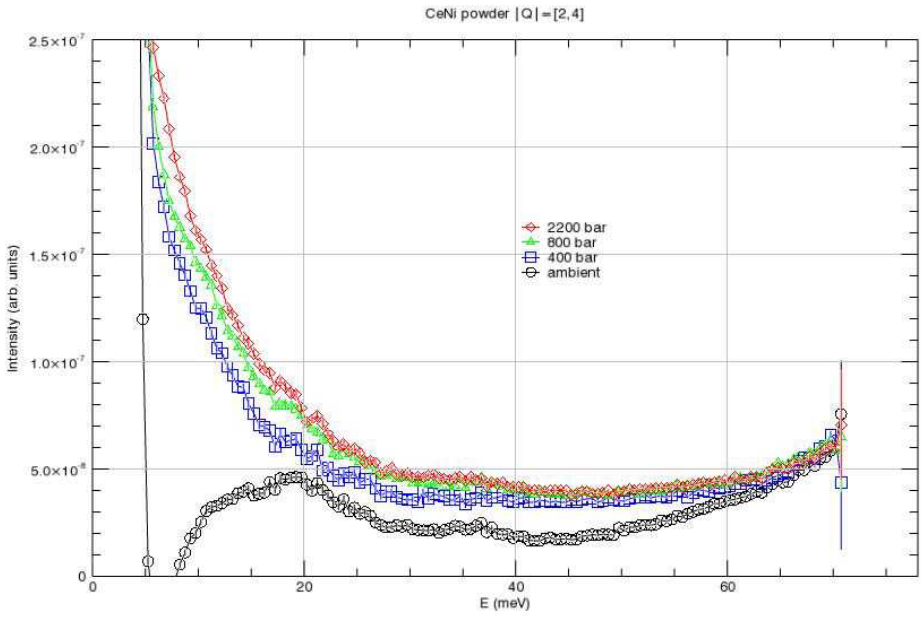

Figure 12. Scattering function S(E) for CeNi averaged over the momentum transfer values 2 < |Q| 4 $Å^{-1}$ at T = 15 K and different pressure values.

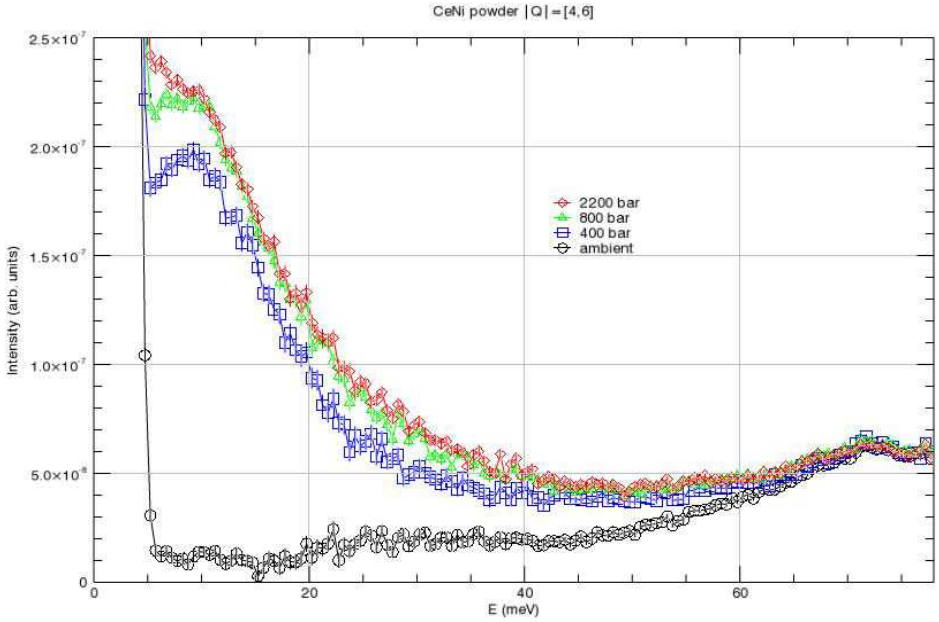

Figure 13. Scattering function S(E) for CeNi averaged over the momentum transfer values 4 < |Q| 6 $Å^{-1}$ at T = 15 K and different pressure values.

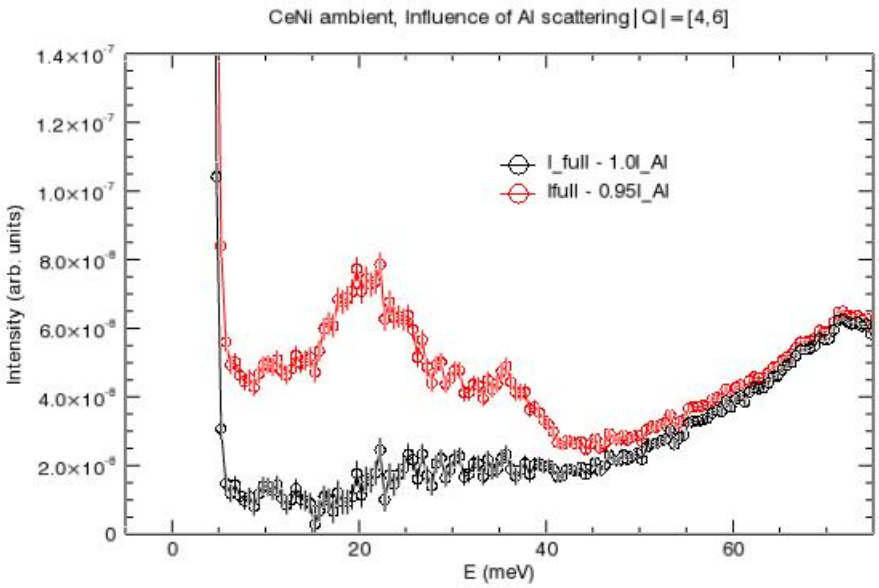

Figure 14. Scattering function S(E) for CeNi averaged over the momentum transfer values 4 < |Q| 6 $Å^{-1}$ at 15 K and ambient pressure. Reducing the background level (= scattering function of the empty pressure cell) only by 5% dramatically changes the "residual" which is the required scattering function of CeNi single crystal.

experimentally using higher neutron incident energy ~ 150 meV. The lack of pronounced CeNi phonon contribution to the scattering intensity at ambient pressure and at high momentum transfer (Fig. 13, energy range between 10 and 30 meV) can be connected with some overestimation of the background. Figure 14 demonstrates the sensitivity of "magnetic" scattering to the level of background subtracted from the measured inelastic signal. Therefore, for the correct interpretation of the inelastic data obtained in the present study it is necessary to have a "reference" CeNi scattering function S(Q,E,T), i.e. CeNi scattering function measured for the same single crystal but out of the pressure cell using two incident neutron energy, 81.8 and ~150 meV. Andrey Podlesnyak and Alexander Kolesnikov plan to perform these additional measurements at the end of February.

A.M. thanks A. Kolesnykov and A. Podlesnyak for their efforts to perform IPTS 8937 INS experiment using fine-resolution Fermi chopper spectrometer SEQUOIA. A.M. specially thanks A.P. for his key contribution to the visualization and treatment of the results obtained as well as for fruitful discussions.

References

1. A.E. Dwight, R.A. Conner, Jr., J.W. Downey, Acta Cryst. **18**, 837 (1965).
2. R. Lemaire and D. Paccard, J. Less-Common Metals **21**, 403 (1970).
3. A. Mirmelstein, E. Clementyev, O. Kerbel, D. Kozlenko, Yu. Akshentsev, V. Voronin, I. Berger, J. Nucl. Mater. **385**, 57 (2009).
4. V.N. Lazukov, E.V. Nefedova, V.V. Sikolenko, U. Staub, P.A. Alekseev, M. Braden, K.S. Nemkovskii, C. Pradervant, I.P. Sadikov, L. Soderholm, N.N. Tiden**,** Appl. Phys. A **74**[Suppl.], S559 (2002).
5. M. Kresch, M. Lucas. O. Delaire, J.Y.Y. Lin, and B. Fultz, Ohys. Rev. B **77**, 024301 (2008).